processes

MDPI

Article

Preparation and Characterization of Furosemide-Silver Complex Loaded Chitosan Nanoparticles

Victor A. Rodriguez [1,2], Pradeep Kumar Bolla [1,2], Rahul S. Kalhapure [1], Sai Hanuman Sagar Boddu [3], Rabin Neupane [3], Julian Franco [1,2] and Jwala Renukuntla [1,*]

1 School of Pharmacy, University of Texas at El Paso, 1101 N. Campbell St, El Paso, TX 79902, USA; varodriguez11@miners.utep.edu (V.A.R.); pbolla@miners.utep.edu (P.K.B.); rkalhapure@utep.edu (R.S.K.); jfranco11@miners.utep.edu (J.F.)

2 Department of Biomedical Engineering, College of Engineering, University of Texas at El Paso, 500 W University Ave, El Paso, TX 79968, USA

3 Department of Pharmacy Practice, The University of Toledo HSC, College of Pharmacy and Pharmaceutical Sciences, 3000 Arlington Ave. (MS1013) Toledo, OH 43614, USA; SaiHanumanSagar.Boddu@utoledo.edu (S.H.S.B.); Rabin.Neupane@rockets.utoledo.edu (R.N.)

* Correspondence: jrenukuntla@utep.edu; Tel.: +1-915-747-8189

Received: 13 February 2019; Accepted: 3 April 2019; Published: 11 April 2019

Abstract: Antibiotic-resistant bacteria may result in serious infections which are difficult to treat. In addition, the poor antibiotic pipeline has contributed to the crisis. Recently, a complex of furosemide and silver (Ag-FSE) has been reported as a potential antibacterial agent. However, its poor aqueous solubility is limiting its activity. The purpose of this study was to encapsulate Ag-FSE into chitosan nanoparticles (CSNPs) and evaluate antibacterial efficacy. Ag-FSE CSNPs were prepared using an ionic gelation technique. The particle size, polydispersity index, and zeta potential of Ag-FSE CSNPs were 197.1 ± 3.88 nm 0.234 ± 0.018 and 36.7 ± 1.78 mV, respectively. Encapsulation efficiency was 66.72 ± 4.14%. In vitro antibacterial activity results showed that there was 3- and 6-fold enhanced activity with Ag-FSE CSNPs against *E. coli* and *S. aureus*, respectively. Results also confirmed that Ag-FSE CSNPs showed ~44% release within 4 h at pH 5.5 and 6.5. Moreover, release from the CSNPs was sustained with a cumulative release of ~75% over a period of 24 h. In conclusion, encapsulation of Ag-FSE into CSNPs resulted in significant improvement of antibacterial efficacy with a sustained and pH-sensitive release. Therefore, Ag-FSE CSNPs can be considered as a potential novel antibacterial agent against bacterial infections.

Keywords: Chitosan nanoparticles; ionic-gelation; antibiotic resistance; furosemide-silver complex; antibacterial; pH-sensitive; staphylococcus aureus

1. Introduction

In today's world, the treatment of infectious diseases is a challenging problem to solve due to the combination of microbial resistance and emerging infections. Antibiotic-resistant bacteria resulted in 2 million infectious diseases in the US annually and nearly 23,000 deaths [1]. One of the first lines of treatment for bacterial infections is antibiotic therapy which has saved millions of lives and treated numerous infectious diseases [2]. Antibiotic-resistant strains of bacteria may result in serious infections or lead to prolonged symptoms which are difficult to treat. Insufficient dosing results in bacteria gaining antibiotic resistance through natural selection and mutations [3]. In addition, the poor antibiotic pharmaceutical pipeline development has contributed to the current crisis [4]. With increasing challenges

in antibiotic therapy, scientists are exploring novel combinations of antibiotics, excipients, and drug delivery carriers. These novel antibiotic drug delivery systems are expected to be less susceptible to bacterial resistance. An approach to developing novel antibiotics is the complexation of antimicrobials to silver (Ag). These antibacterial metal complexes can be further developed into nanoparticulate formulations for sustained and targeted release. Silver (Ag) exhibits antibacterial activity via multiple mechanisms of action which result in decreased bacterial resistance [5]. Previously known complexes include silver sulfadiazine and clotrimazole silver complex [6,7]. Recently, a complex of silver and furosemide (Ag-FSE) has been developed as an antibacterial agent, however, it has poor aqueous solubility [8]. The poor solubility problem associated with Ag-FSE can be resolved using nano drug delivery systems such as nanosuspensions, nano micelles, liposomes, and solid lipid nanoparticles [9–12]. In recent years, chitosan (CS) has been widely used in the areas of bioengineering, biopharmaceuticals, and nanomedicine for the development of efficient drug delivery systems [13]. CS is a synthetically produced biopolymer produced through a deacetylation process of chitin, a naturally occurring biopolymer in exoskeletons of insects, crustaceans, and fungi [14]. CS is biocompatible, biodegradable, and tunable for drug encapsulation and controlled drug release. Nowadays CS-based formulations have made substantial breakthroughs and are being studied for clinical applications. A spray dried powder composed of CS and norovirus VLP antigen was administered intranasally in a phase 1 clinical study. Results from this study showed increased immune response with no adverse vaccine effects after an evaluation period of 180 days [15]. It has also been reported that CS-based preparations have been used in dental practices (mouthwashes, toothpastes, and hemostats) [16–18]. A currently underway clinical study is evaluating the effect of CS nanoparticles-based gel formulations delivered by the intracanal route to treat root canal bacterial infections in primary teeth [19]. Considering the advantages with CS, we hypothesize that chitosan nanoparticles loaded with Ag-FSE can improve solubility and antibacterial activity. The formulated of Ag-FSE CSNPs were characterized for size, zeta potential, polydispersity index, encapsulation efficiency (EE%), and evaluated for antibacterial activity and stability.

2. Materials and Methods

2.1. Materials

Furosemide was purchased from Acros Organics (NJ, USA). Chitosan, 85% deacetylated powder was procured from Alfa Aesar (Ward Hill, MA, USA). Silver nitrate (AgNO3), potassium hydroxide (KOH), sodium triphosphate (TPP), dimethyl sulfoxide (DMSO), buffer salts, acetic acid and methanol (ACS grade) were obtained from Fisher Scientific (Fair Lawn, NJ, USA). Deionized water used in experiments was obtained from in-house Milli-Q® IQ 7000 Ultrapure Water System (Millipore, Bedford, MA, USA). Dialysis tubing with MWCO of 14,400 was procured from Sigma-Aldrich®(St. Louis, MO, USA). Muller-Hinton broth (CM0405) was obtained from Oxoid Microbiology Products, bacterial strains were purchased from the American Type Culture Collection (ATCC), and sterile microtiter plates were procured from Fisher Scientific (Fair Lawn, NJ, USA).

2.2. Methods

2.2.1. Synthesis of Ag-FSE Complex

Synthesis of the Ag-FSE complex was performed as reported by Lustri et al. 2017 with minor modifications to the procedure (Scheme 1) [8]. Briefly, an aqueous solution (2 mL) of $AgNO_3$ (0.362 g, 2.13 mmol) was added dropwise into a methanolic solution (20 mL) of furosemide (0.704 g, 2.13 mmol) and KOH (0.119 g, 2.13 mmol) under stirring. This reaction mixture was then subjected to continuous stirring at room temperature for 2 h, and a final product of white precipitate was collected by filtration. The white precipitate of Ag-FSE Complex was then washed with cold water three times and dried in a desiccator overnight under negative pressure for 24 h.

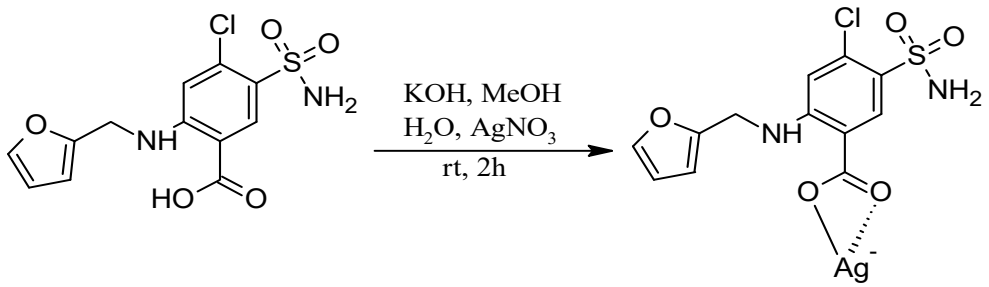

Scheme 1. Synthesis of the Ag-FSE complex.

2.2.2. Preparation of CSNPs

CSNPs were formulated by an ionic gelation technique as described by Kalhapure et al. 2017 with slight modifications, for both blank and Ag-FSE loaded nanoparticles [20]. Blank CSNPs were prepared as such; CS solution (10 mL) (1% w/v in 1% acetic acid) was kept under stirring at 1000 rpm for 10 min followed by dropwise addition of 0.1% w/v TPP solution (20 mL) under continuous stirring. The resultant solution was kept under stirring for 5 min after the addition of all TPP solution. The pH of the final solution was adjusted to 5.5 with 0.5 M NaOH. Following this, the formulation was sonicated at 30% amplitude using probe sonicator (Fisher scientific TM Model 505 Sonic Dismembrator) in an ice bath. Thereafter, the formulation was stirred at 1000 rpm for 20 min in the dark. Ag-FSE loaded CSNPs were prepared using the same method as blank CSNPs. A weighed amount of the Ag-FSE complex was added into the TPP solution (20 mL) and then subjected to probe sonication at 30% amplitude. The homogenous Ag-FSE-TPP solution was then added dropwise into CS solution (10 mL) and processed further as the blank CSNPs to obtain Ag-FSE loaded CSNPs.

2.2.3. Determination of Size, Polydispersity Index (PDI), and Zeta Potential (ZP)

The size, PDI, and ZP analysis of the CSNPs was performed using dynamic light scattering (DLS) technique. CSNPs (100 µl) were dispersed in deionized water (10 mL) and measurements were performed with a Zetasizer Nano ZS90 (Malvern Zetasizer Nano ZS90, Malvern Instrument Ltd., Malvern, WR, UK) at 25 °C and 90° scattering angle.

2.2.4. Drug Encapsulation Efficiency (EE%)

Drug-loaded Ag-FSE CSNP encapsulation efficiency was determined using a modified ultrafiltration technique [21,22]. Ag-FSE loaded CSNPs (500 µl) were pipetted into Ultracel®centrifugal filter units with an MWCO of 10 kDa. These samples were then centrifuged at 10,000 rpm (accuSpin Micro 17R, Fisher Scientific) for 30 min at 20 °C allowing for the separation of the unentrapped drug from the encapsulated drug. After centrifugation, the filtrate was collected and 300 µl was diluted to 3 mL with milli-Q water and analyzed using UV-spectrophotometer (UV-vis) (Shimadzu UV-1800, Japan) at max = 277 nm. The regression equation used for calculations was y = 0.0486x + 0.0135 with R2 = 0.9995. The following equation was used to determine the EE% of the CSNPs: EE% = (Total drug − Free drug)/(Total drug) × 100.

2.2.5. Transmission Electron Microscopy (TEM)

Transmission electron microscopy (TEM) (HITACHI HD-2300 A, Ultrathin Film Evaluation System by Hitachi High Technologies America, Pleasanton, CA, USA) was used to assess surface morphology of the Ag-FSE loaded CSNPs. A liquid sample of Ag-FSE CSNPs was placed on a copper platform and left overnight. TEM images were visualized at an accelerating voltage of 200 kV.

2.2.6. X-Ray Diffraction (XRD)

XRD analysis of the Ag-FSE CSNPs was performed using PANanlytical's X-ray diffractometer (PANanlytical's X'pert Pro Tokyo, Japan) equipped with an X'Celerator high-speed detector. XRD studies were performed for CS, TPP, Ag-FSE and Ag-FSE CSNPs. Powdered samples were placed on an aluminum sample holder and uniformly packed using glass slides. The radiation source was CuKα operated at 45 kV and 40 mA. All the measurements were recorded with continuous scanning mode over a 2θ range of 5° to 70°.

2.2.7. Differential Scanning Calorimetry (DSC)

DSC analysis for Ag-FSE CSNPs, Ag-FSE and CS were performed using a DSC Q20 instrument with TA universal analysis software to obtain scans. Samples (5–10 mg) were placed in aluminum pans and sealed. DSC analysis was performed at a heating rate of 10 °C/min over a range of 40 °C to 300 °C with a nitrogen flow of 20 mL/min.

2.2.8. In Vitro Drug Release Studies

Drug release behavior from the CSNPs and free drug (Ag-FSE) in phosphate buffer saline (PBS) (pH 7.4, 6.5 and 5.5) was evaluated using dialysis the bag method (MW 8000–14,400 Da) [23,24]. Briefly, 3 mL of Blank CSNPs and Ag-FSE CSNPs (~1 mg Ag-FSE) in PBS were transferred into separate dialysis bags. These dialysis bags were placed in conical tubes (50 mL capacity) containing 30 mL of PBS as the release medium (pH 7.4, 6.5 and 5.5) maintained at 37 ± 0.5 °C in a shaking water bath (100 rpm). At a pre-determined time intervals, 3 mL of the samples were collected from the conical tubes and replaced with 3 mL of fresh PBS to maintain sink conditions. Pre-determined time intervals were 0.5, 1, 2, 3, 4, 5, 6, 7, 8, and 24 h. The amount of drug released from the formulations at different timepoints was quantified using a UV-visible spectrophotometer (Shimadzu UV 1800, Japan) at λmax of 277 nm. All the experiments were performed in triplicate.

2.2.9. In Vitro Antibacterial Activity

Ag-FSE loaded CSNPs and free Ag-FSE were evaluated for antibacterial activity against *E. coli* (ATCC25922) and *S. aureus* (ATCC25923) using a broth microdilution method. Colonies of each bacterial strain were grown overnight in Muller-Hinton broth (MHB) in an incubator at 37 °C. Single bacterial culture colonies of each bacterium were suspended in MHB and further diluted with MHB until a cell density of 0.5 Mcfarland for each bacterium was attained. Diluted bacterial suspensions (100 µL) were transferred into 96-well plates. Upon seeding with the designated bacteria, serial dilutions of 100 µL of Ag-FSE CSNPs, blank CSNPs, free Ag-FSE in 10% w/v DMSO, MHB, and plain 10% DMSO were performed. Plates were incubated overnight at 37 °C and minimum inhibitory concentration (MIC) was assessed as the concentration at which no bacterial growth was observed. All experiments were completed in triplicate.

2.2.10. Stability Studies

Three batches of Ag-FSE CSNPs were prepared under optimum conditions and their size, PDI, and ZP were analyzed. Thereafter, the samples were stored at 25 °C and 4 °C conditions. Stability was assessed using DLS analysis for four months (120 days). The parameters monitored to assess the stability were physical appearance, size, PDI, and ZP.

2.2.11. Statistical Analysis

Statistical analysis was performed using a t-test followed by Bonferroni's multiple comparison test using GraphPad Prism®(Graph Pad Software Inc., Version 5.0, San Diego, CA, USA). A p-value < 0.05 was considered statistically significant.

3. Results and Discussion

3.1. Characterization of CSNPs

3.1.1. Effect of Sonication Time on Blank and Ag-FSE CSNPs

Blank CSNPs and Ag-FSE CSNPs were formulated using an ionic gelation technique. The effect of sonication time on the size, PDI and ZP of CSNPs was studied. Table 1 and Figure 1 summarize the effect of sonication time (3, 5, 10 and 20 min at 30% amplitude) on size, PDI, and ZP on blank CSNPs. Size, PDI, and ZP of blank CSNPs ranged from 204.8 ± 4.43–472.1 ± 42.81, 0.195 ± 0.023–0.517 ± 0.107, and 36.0 ± 2.54–44.1 ± 2.21 respectively. It was observed that with increasing sonication time there was a significant decrease in particle size from 3–10 min, however, at 10 min and 20 min there was no significant difference ($p > 0.05$) in particle size. Thus, 10 min of sonication was considered as the optimum sonication time for preparing CSNPs with <300 nm size, low PDI, and high ZP. Low PDI and high ZP of CSNPs suggest that the system was monodisperse and electrostatically stable. Similar results were observed by Tang et al. where the increase in sonication time caused the cleaving of free unpolymerized chitosan, reducing particle size and enhancing the monodispersity of the system [25].

Table 1. Effects of sonication time on size, polydispersity index (PDI), and zeta potential (ZP) of blank chitosan nanoparticles (CSNPs).

Time (min)	Size (nm)	PDI	ZP (mV)
3	344.6 ± 98.9	0.517 ± 0.107	44.1 ± 2.21
5	472.1 ± 42.8	0.507 ± 0.139	42.9 ± 3.86
10	261.3 ± 12.2	0.195 ± 0.023	42.8 ± 1.31
20	204.8 ± 4.4	0.205 ± 0.019	36.0 ± 2.54

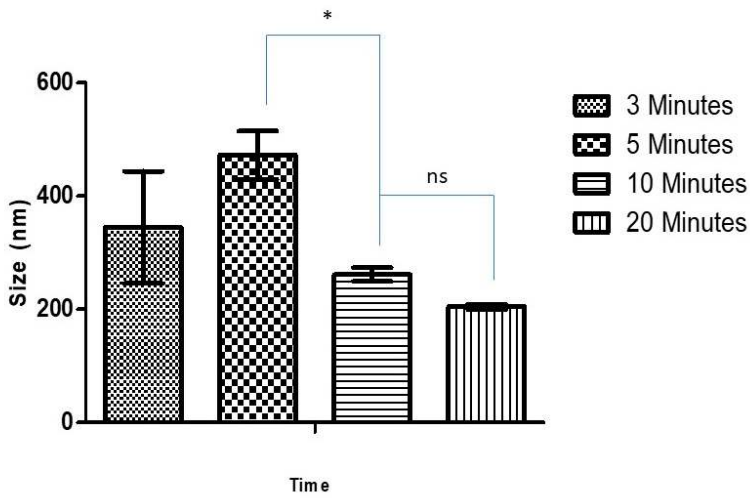

Figure 1. Effect of sonication time on size of blank CSNP; * significant difference with CSNP size at 5 and 10 min sonication ($p < 0.05$); ns, non-significant.

After optimizing the sonication time for blank CSNPs, the effect of sonication time on the size of Ag-FSE CSNPs was studied. Initially, 5 mg Ag-FSE was loaded into the CSNPs and analyzed for differences in size, PDI, and ZP with respect to 5 and 10-minute sonication times. The effect of sonication time on the size, PDI, and ZP of Ag-FSE CSNP is provided in Table 2 and Figure 2. Results confirmed that there was a significant difference with respect to size between 5 min and 10 min of sonication ($p < 0.05$). Therefore, 10 min was considered as the optimum sonication time for both blank and Ag-FSE CSNPs.

Table 2. Effects of sonication time on CSNPs loaded with 5 mg of Ag-FSE.

Time (min)	Size (nm)	PDI	ZP (mV)
5	481.4 ± 28.9	0.520 ± 0.100	42.2 ± 2.44
10	210.5 ± 3.11	0.232 ± 0.009	41.5 ± 3.39

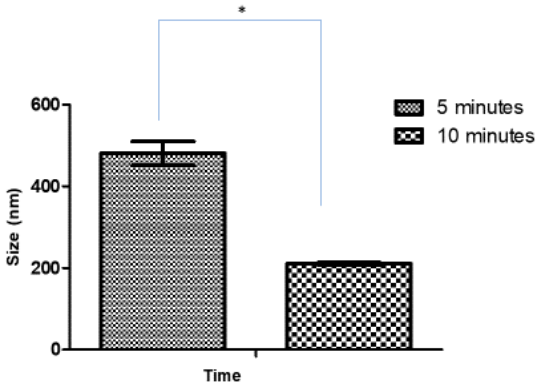

Figure 2. Effect of sonication time on the size of Ag-FSE CSNPs (5mg); *significant difference with CSNP sizes ($p < 0.05$).

3.1.2. Effect of Drug Loading on Size, PDI, and ZP of Ag-FSE CSNPs

After the preliminary studies, 10 min was considered the optimum sonication time for the formulation of Ag-FSE CSNPs. The effect of increased drug loading (10 mg) on the size, PDI, and ZP of Ag-FSE was studied and summarized in Table 3 and Figure 3. Interestingly, it was found that the increase in Ag-FSE loading from 5–10 mg resulted in CSNPs with a significantly smaller particle size ($p < 0.05$). The size, PDI, and ZP of 10 mg loaded Ag-FSE CSNPs were 197.1 ± 3.88 nm 0.234 ± 0.018 and 36.7 ± 1.78 mV, respectively. The low PDI values and high ZP indicate that under 10-minute sonication with 10 mg loaded into the CSNPs continued to exhibit monodispersity and electrostatic stability for an optimized drug delivery system. With higher Ag-FSE loading, the size of the CSNPs will remain optimal with <300 nm sizes as no significant differences ($p > 0.05$) were observed when investigating if size being affected by higher concentrations.

Table 3. Effects of drug loading on size, PDI, and ZP of CSNPs.

Ag-FSE loading (mg)	Size (nm)	PDI	ZP (mV)
5	210.5 ± 3.11	0.232 ± 0.009	41.5 ± 3.39
10	197.1 ± 3.88	0.234 ± 0.018	36.7 ± 1.78

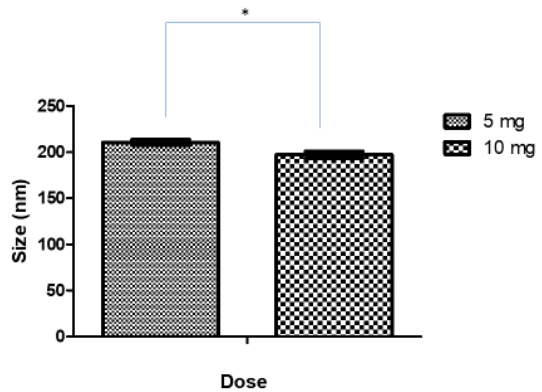

Figure 3. Effect of drug loading on size of CSNPs; * significant difference between 5 mg and 10 mg loading ($p < 0.05$).

3.2. Drug Encapsulation Efficiency (EE%)

Ag-FSE CSNPs showed high encapsulation with EE% of 66.72 ± 4.14%. The high EE% for Ag-FSE could be attributed to the electrostatic nature of the two constituents, CS being cationic, while the Ag-FSE complex holds an anionic nature, allowing for the polymerization of CS and formulation of the nanoparticles with the loaded drug [26].

3.3. Transmission Electron Microscopy

TEM images of the Ag-FSE CSNPs indicated that the nanoparticles were globular in shape (Figure 4). Analysis of the Ag-FSE CSNP morphology also showed that a decrease in particle size occurred when compared to DLS results due to dehydration of the particles when undergoing TEM analysis.

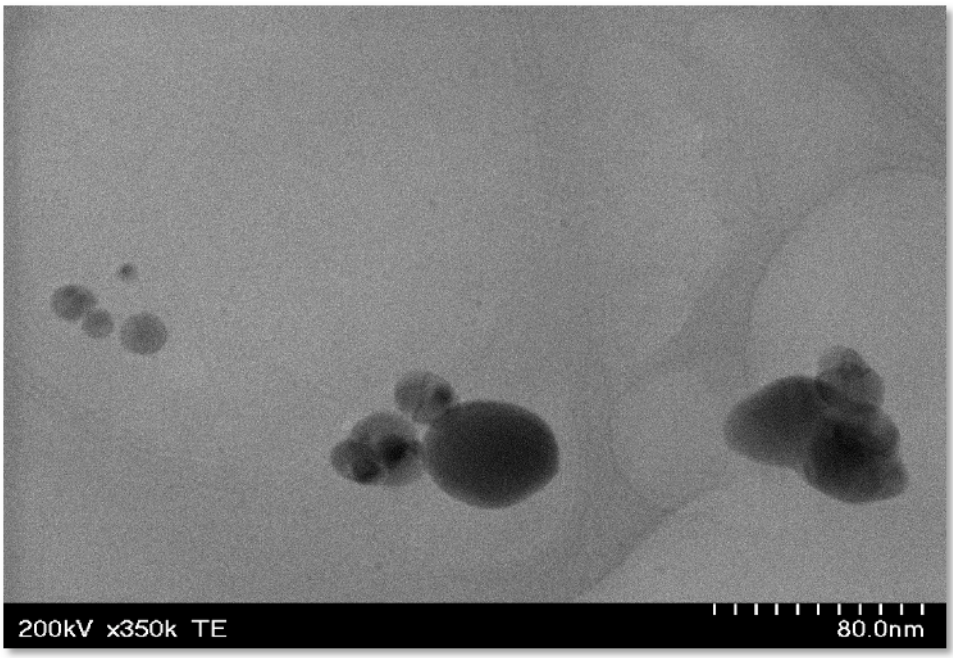

Figure 4. TEM images of Ag-FSE loaded CSNPs; where nanoparticles appeared globular in shape.

3.4. XRD Analysis

As silver complexes are inherently reported to have poor aqueous solubility [6], it is crucial to study the crystalline nature of the formulation. The crystalline nature of the drug can affect the solubility, stability, and bioavailability. XRD was performed for Ag-FSE, CS, and Ag-FSE CSNPs to confirm the crystalline nature. Results show that Ag-FSE exhibited a crystalline nature with characteristic peaks at 6.18, 10.28, 18.48, 25.92, and 32.8 °C. However, when Ag-FSE was encapsulated into CSNPs, it was observed that Ag-FSE had undergone a phase transition from a crystalline to an amorphous state (Figure 5). The transition can be confirmed by the absence of the characteristic peaks of Ag-FSE in the XRD of Ag-FSE CSNPs (Figure 5c). Similar findings were observed with other CSNP formulations [27].

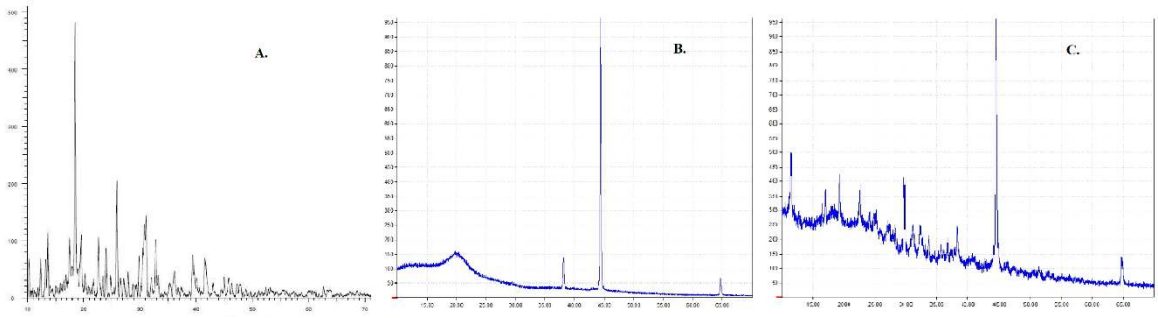

Figure 5. XRD results for (**a**) plain Ag-FSE, (**b**) plain chitosan (CS), and (**c**) Ag-FSE CSNPs.

3.5. DSC of Ag-FSE CSNPs

The phase transition of Ag-FSE from crystalline to amorphous form was further confirmed by DSC. DSC evaluates the melting and crystalline behavior of drugs. DSC results of Ag-FSE, CS, and Ag-FSE CSNPs are provided in Figure 6. Results show that Ag-FSE showed a sharp exothermic peak at 211.69 °C. However, the characteristic exothermic peak of Ag-FSE was absent in the DSC of Ag-FSE CSNPs, confirming the encapsulation of Ag-FSE into CSNPs.

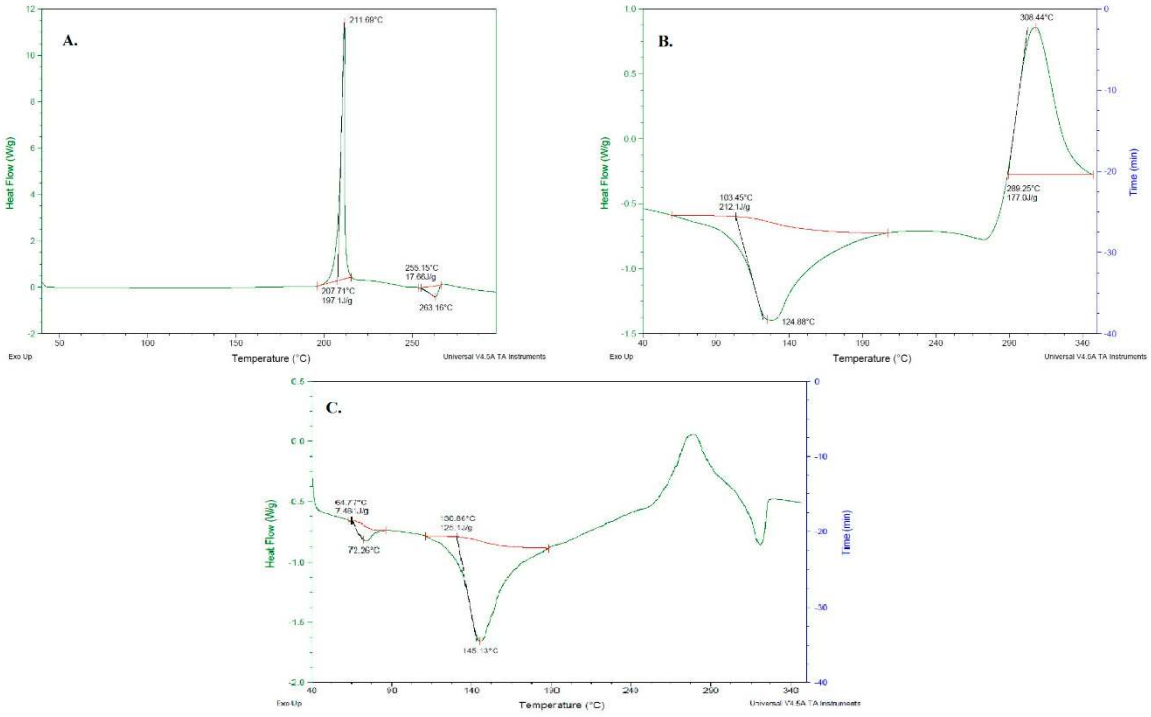

Figure 6. DSC results of (**a**) Ag-FSE, (**b**) CS and (**c**) Ag-FSE CSNPs.

3.6. In Vitro Drug Release Studies

Ag-FSE encapsulated CSNPs showed sustained release with a cumulative release of ~75% over a period of 24 h. In vitro drug release profiles of Ag-FSE CSNPs and free Ag-FSE are provided in Figure 7. As bacterial infections are associated with varying pHs at the infection site, release profiles at physiological pH (7.4) and acidic pH (6.5 and 5.5) were also studied (Figure 7). Ag-FSE CSNPs showed sustained and controlled release over a period of 24 h at all pHs. At pH 5.5 and 6.5, the CSNPs had an initial burst like release during the first 4 h with a cumulative release ranging from 41.78%–70.57%. This initial burst release could be due to unencapsulated Ag-FSE molecules that remained along the surface of the CSNPs [22]. It was observed that at pH 5.5 and 6.5, ~ 42%–44% of Ag-FSE was released

within 0.5 h, whereas at pH 7.4, only a ~29% release was observed in the first 0.5 h. A similar release profile was observed with CS under acidic conditions reported in the literature [23].

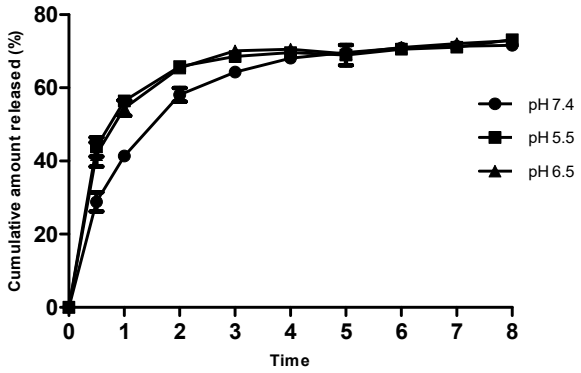

Figure 7. In vitro release profile of Ag-FSE CSNPs at pH 7.4, 5.5 and 6.5. Data are expressed in mean ± SD (n = 3).

3.7. In Vitro Antibacterial Activity

In vitro antibacterial activity was assessed using a broth microdilution method. Results showed that Ag-FSE CSNPs exhibited significantly greater inhibitory activity against *E. Coli* and *S. aureus* compared to Ag-FSE. Against *E. coli*; the MIC of Ag-FSE was 166.5 µg/mL, whereas the value for plain Ag-FSE was 500 µg/mL. There was a 6-fold enhancement in activity against *S. aureus* (Table 4). The MIC values suggested that the Ag-FSE loaded CSNP formulation had notably greater antibacterial activity compared to the unencapsulated drug. Blank CSNPs exhibited a very low antibacterial activity, however, the results were incomparable to the Ag-FSE loaded CSNPs. Although blank CSNPs showed low antibacterial activity, the results for Ag-FSE loaded CSNPs may suggest synergistic activity due to CS being a bioactive polymer with antibiofilm and antimicrobial properties [28]. Results confirmed that encapsulation of Ag-FSE into CSNPs enhanced the antibacterial efficiency of Ag-FSE.

Table 4. Minimum inhibition concentrations for blank CSNP, Ag-FSE CSNP, Ag-FSE-10%, DMSOm and 10% DMSO against *E. coli* and *S. aureus* (n = 3).

Formulation	Minimum Inhibition Concentration (µg/mL)	
	E. coli	*S. aureus*
Blank CSNPs	NA	NA
Ag-FSE CSNPs	166.5	41.63
Ag-FSE 10% DMSO	500	250
10% DMSO	NA	NA

3.8. Stability Studies

Stability studies were performed for both 5 mg and 10 mg loaded Ag-FSE CSNPs over 120 days. Size, PDI, and ZP were investigated to confirm the physical stability of CSNPs. Formulations were stored at 4 °C and 25 °C and analyzed over the course of time (days 0, 30, 60 and 120). Stability study results for 5 mg and 10 mg loaded CSNPs are provided in Tables 5 and 6, respectively. Results showed that there was a steady decrease in the size of the 5 mg loaded Ag-FSE CSNPs from days 30–60. The decreased size may be due to the cationic and anionic interactions of CS and Ag causing the particle size to decrease [29]. Also, 10 mg loaded Ag-FSE CSNPs stored at 25 °C showed a slight increase in size for 4 °C. Day 120 analysis indicated an increase in particle size for both 5 mg and 10 mg loaded Ag-FSE CSNPs. The increased size may be due to particle aggregation or swelling caused by changes in environmental conditions (temperature, pH, ionic strength) [30]. The overall difference in size, PDI,

and ZP of all the samples at different time points was not significant ($p > 0.05$). Therefore, formulations can be considered stable at 25 °C and 4 °C for 120 days.

Table 5. Effect of storage on particle size, PDI, and ZP of 5 mg loaded CSNPs for 30, 60, and 120 days at 4 °C and 25 °C.

Storage Time	Size (nm)		PDI		ZP (mV)	
	4 °C	25 °C	4 °C	25 °C	4 °C	25 °C
Day 0	290.3 ± 162.6		0.395 ± 0.222		35.5 ± 1.52	
Day 30	239.8 ± 9.8	241.5 ± 5.6	0.224 ± 0.023	0.191 ± 0.021	33.7 ± 1.70	35.6 ± 1.08
Day 60	229.7 ± 3.2	232.0 ± 11.2	0.217 ± 0.008	0.242 ± 0.018	39.0 ± 2.09	35.5 ± 8.90
Day 120	296.8 ± 2.8	331.8 ± 16.1	0.236 ± 0.014	0.288 ± 0.038	29.8 ± 2.03	30.7 ± 0.66

Table 6. Effect of storage on particle size, PDI, and ZP of 10 mg loaded CSNPs for 30, 60 and 120 days at 4 °C and 25 °C.

Storage Time	Size (nm)		PDI		ZP (mV)	
	4 °C	25 °C	4 °C	25 °C	4 °C	25 °C
Day 0	216.6 ± 26.8		0.194 ± 0.021		25.8 ± 3.05	
Day 30	224.6 ± 13.8	176.5 ± 10.5	0.217 ± 0.025	0.272 ± 0.030	30.5 ± 11.1	30.3 ± 5.45
Day 60	217.4 ± 5.3	207.3 ± 9.9	0.232 ± 0.017	0.248 ± 0.018	37.3 ± 3.79	36.2 ± 6.61
Day 120	324.8 ± 50.7	321.7 ± 33.5	0.587 ± 0.162	0.407 ± 0.021	39.7 ± 1.92	37.3 ± 2.40

4. Conclusions

In the present study, we successfully encapsulated a novel antibacterial complex, Ag-FSE, into CSNPs for enhancement in its antibacterial efficacy. The size of the formulated Ag-FSE CSNPs was <300 nm with high %EE of ~66%. Ag-FSE CSNPs were globular in shape with smooth surfaces. XRD and DSC confirmed the transition of Ag-FSE from crystalline to amorphous form when formulated as Ag-FSE CSNPs. Ag-FSE CSNPs showed significant antibacterial activity against *E. Coli* (Gram-negative) an *S. aureus* (Gram-positive) bacteria. Stability studies indicated that the Ag-FSE CSNPs at 4 °C and 25 °C conditions remained stable over 120 days. Further exploration of developed CSNPs with in-depth in vivo studies could lead to its further transition to clinical trials.

Author Contributions: Conceptualization, J.R. and R.S.K.; methodology, V.A.R., P.K.B., J.F., R.N.; formal analysis, V.A.R., P.K.B. writing—original draft preparation, V.A.R., P.K.B.; writing—review and editing, J.R., R.S.K., S.H.S.B.

Acknowledgments: The authors are thankful to Delfina Dominguez for providing facility to perform antibacterial activity studies.

Conflicts of Interest: The authors declare no conflict of interest.

References

1. Centers for Disease Control and Prevention, Antibiotic/Antimicrobial Resistance, (n.d.). Available online: https://www.cdc.gov/drugresistance/index.html (accessed on 19 July 2018).
2. Adedeji, W.A. The Treasure Called Antibiotics. *Ann. Ib. Postgrad. Med.* **2016**, *14*, 56–57. [PubMed]
3. Richardson, L.A. Understanding and overcoming antibiotic resistance. *PLoS Biol.* **2017**, *15*, 1–5. [CrossRef]
4. Faya, M.; Kalhapure, R.S.; Kumalo, H.M.; Waddad, A.Y.; Omolo, C.; Govender, T. Conjugates and nano-delivery of antimicrobial peptides for enhancing therapeutic activity. *J. Drug Deliv. Sci. Technol.* **2018**, *44*, 153–171. [CrossRef]
5. Keller, A.A.; Adeleye, A.S.; Conway, J.R.; Garner, K.L.; Zhao, L.; Cherr, G.N.; Hong, J.; Gardea-Torresdey, J.L.; Godwin, H.A.; Hanna, S.; et al. Comparative environmental fate and toxicity of copper nanomaterials. *NanoImpact* **2017**, *7*, 28–40. [CrossRef]

6. Clement, J.L.; Jarrett, P.S. Antibacterial Silver. *Met. Based Drugs* **1994**, *1*, 467–482. [CrossRef] [PubMed]
7. Kalhapure, R.S.; Sonawane, S.J.; Sikwal, D.R.; Jadhav, M.; Rambharose, S.; Mocktar, C.; Govender, T. Solid lipid nanoparticles of clotrimazole silver complex: An efficient nano antibacterial against Staphylococcus aureus and MRSA. *Colloids Surf. B Biointerfaces* **2015**, *136*, 651–658. [CrossRef] [PubMed]
8. Lustri, B.C.; Massabni, A.C.; Silva, M.A.C.; Nogueira, F.A.R.; Aquino, R.; Amaral, A.C.; Massabni, A.C.; Barud, H.d. Spectroscopic characterization and biological studies in vitro of a new silver complex with furosemide: Prospective of application as an antimicrobial agent. *J. Mol. Struct.* **2017**, *1134*, 386–394. [CrossRef]
9. Shakhashiri, B.Z.; Dirreen, G.E.; Juergens, F. Color, solubility, and complex ion equilibria of nickel(II) species in aqueous solution. *J. Chem. Educ.* **1980**, *57*, 900. [CrossRef]
10. Kalepu, S.; Nekkanti, V. Insoluble drug delivery strategies: Review of recent advances and business prospects. *Acta Pharm. Sin. B.* **2015**, *5*, 442–453. [CrossRef] [PubMed]
11. Bolla, P.K.; Kalhapure, R.S.; Rodriguez, V.A.; Ramos, D.V.; Dahl, A.; Renukuntla, J. Preparation of solid lipid nanoparticles of furosemide-silver complex and evaluation of antibacterial activity. *J. Drug Deliv. Sci. Technol.* **2019**, *49*, 6–13. [CrossRef]
12. Renukuntla, J. FSE–Ag complex NS: Preparation and evaluation of antibacterial activity. *Iet Nanobiotechnology* **2018**, 1–5. [CrossRef]
13. Ghadi, A.; Mahjoub, S.; Tabandeh, F.; Talebnia, F. Synthesis and optimization of chitosan nanoparticles: Potential applications in nanomedicine and biomedical engineering. *Casp. J. Intern. Med.* **2014**, *5*, 156–161.
14. Dash, M.; Chiellini, F.; Ottenbrite, R.M.; Chiellini, E. Chitosan—A versatile semi-synthetic polymer in biomedical applications. *Prog. Polym. Sci.* **2011**, *36*, 981–1014. [CrossRef]
15. Mohammed, M.A.; Syeda, J.T.M.; Wasan, K.M.; Wasan, E.K. An overview of chitosan nanoparticles and its application in non-parenteral drug delivery. *Pharmaceutics* **2017**, *9*, 53. [CrossRef] [PubMed]
16. Wieckiewicz, M.; Boening, K.W.; Grychowska, N.; Paradowska-Stolarz, A. Clinical Application of Chitosan in Dental Specialities. *Mini Rev. Med. Chem.* **2017**, *17*, 401–409. [CrossRef] [PubMed]
17. Kmiec, M.; Pighinelli, L.; Tedesco, M.F.; Silva, M.M.; Reis, V. Chitosan-Properties and Applications in Dentistry. *Adv. Tissue Eng. Regen. Med. Open Access.* **2017**, *2*, 205–211. [CrossRef]
18. Uraz, A.; Boynueğri, D.; Özcan, G.; Karaduman, B.; Uç, D.; Şenel, S.; Pehlivan, S.; Öğüs, E.; Sultan, N. Two percent chitosan mouthwash: A microbiological and clinical comparative study. *J. Dent. Sci.* **2012**, *7*, 342–349. [CrossRef]
19. Chitosan, N.A. Chitosan Nanoparticles, and Chlorhexidine Gluconate, as Intra Canal Medicaments in Primary Teeth, (n.d.). Available online: https://clinicaltrials.gov/ct2/show/NCT03588351 (accessed on 3 July 2018).
20. Kalhapure, R.S.; Jadhav, M.; Rambharose, S.; Mocktar, C.; Singh, S.; Renukuntla, J.; Govender, T. pH-responsive chitosan nanoparticles from a novel twin-chain anionic amphiphile for controlled and targeted delivery of vancomycin. *Colloids Surf. B Biointerfaces* **2017**, *158*, 650–657. [CrossRef]
21. Abdelkader, A.; El-Mokhtar, M.A.; Abdelkader, O.; Hamad, M.A.; Elsabahy, M.; El-Gazayerly, O.N. Ultrahigh antibacterial efficacy of meropenem-loaded chitosan nanoparticles in a septic animal model. *Carbohydr. Polym.* **2017**, *174*, 1041–1050. [CrossRef]
22. Sun, L.; Chen, Y.; Zhou, Y.; Guo, D.; Fan, Y.; Guo, F.; Zheng, Y.; Chen, W. Preparation of 5-fluorouracil-loaded chitosan nanoparticles and study of the sustained release in vitro and in vivo. *Asian J. Pharm. Sci.* **2017**, *12*, 418–423. [CrossRef]
23. Pan, Y.; Li, Y.J.; Zhao, H.Y.; Zheng, J.M.; Xu, H.; Wei, G.; Hao, J.S.; de Cui, F. Bioadhesive polysaccharide in protein delivery system: Chitosan nanoparticles improve the intestinal absorption of insulin in vivo. *Int. J. Pharm.* **2002**, *249*, 139–147. [CrossRef]
24. Liu, H.; He, J. Simultaneous release of hydrophilic and hydrophobic drugs from modified chitosan nanoparticles. *Mater. Lett.* **2015**, *161*, 415–418. [CrossRef]
25. Tang, E.S.K.; Huang, M.; Lim, L.Y. Ultrasonication of chitosan and chitosan nanoparticles. *Int. J. Pharm.* **2003**, *265*, 103–114. [CrossRef]
26. Guibal, E. Interactions of metal ions with chitosan-based sorbents: A review. *Sep. Purif. Technol.* **2004**, *38*, 43–74. [CrossRef]
27. Qi, L.; Xu, Z. Lead sorption from aqueous solutions on chitosan nanoparticles. *Colloids Surf. A Physicochem. Eng. Asp.* **2004**, *251*, 183–190. [CrossRef]

28. Costa, E.M.; Silva, S.; Vicente, S.; Neto, C.; Castro, P.M.; Veiga, M.; Madureira, R.; Tavaria, F.; Pintado, M.M. Chitosan nanoparticles as alternative anti-staphylococci agents: Bactericidal, antibiofilm and antiadhesive effects. *Mater. Sci. Eng. C* **2017**, *79*, 221–226. [CrossRef]
29. Wang, J.J.; Zeng, Z.W.; Xiao, R.Z.; Xie, T.; Zhou, G.L.; Zhan, X.R.; Wang, S.L. Recent advances of chitosan nanoparticles as drug carriers. *Int. J. Nanomed.* **2011**, *6*, 765–774. [CrossRef]
30. López-León, T.; Carvalho, E.L.S.; Seijo, B.; Ortega-Vinuesa, J.L.; Bastos-González, D. Physicochemical characterization of chitosan nanoparticles: Electrokinetic and stability behavior. *J. Colloid Interface Sci.* **2005**, *283*, 344–351. [CrossRef]